Minerals Engineering 216 (2024) 108853

Contents lists available at ScienceDirect

Minerals Engineering

journal homepage: www.elsevier.com/locate/mineng

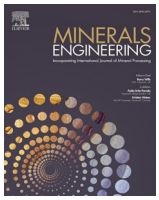

Concurrent leaching of copper and cobalt from a copper–cobalt ore using sulfuric and organic acids

Emmanuel A. Oke [a,*], Herman Potgieter [a,b], Fortune Mondlane [a], Noluthando P. Skosana [a], Samaneh Teimouri [a], Joseph K. Nyembwe [a]

[a] Sustainable and Innovative Minerals and Metals Extraction Technology (SIMMET) Research Group, School of Chemical and Metallurgical Engineering, University of the Witwatersrand Johannesburg, Private Bag X3 PO Wits 2050, Johannesburg, South Africa
[b] Department of Natural Science, Manchester Metropolitan University, Chester Street, Manchester M1 5GD, United Kingdom

ARTICLE INFO

Keywords:
Acid leaching
Citric Acid, Oxalic Acid
Shrinking Core Model
Arrhenius' Law
Activation Energy

ABSTRACT

A study involving the leaching of Cu and Co from a Cu—Co ore in sulfuric acid (H_2SO_4), citric acid (CA) and oxalic acid (OA) using hydrogen peroxide (H_2O_2) as oxidant, was carried out. The ore was characterised by x-ray fluorescence (XRF), x-ray diffraction (XRD) and scanning electron microscopy coupled with energy-dispersive x-ray spectroscopy (SEM-EDX). The results obtained indicate that increasing the time, temperature, and concentration of the leaching agent/oxidant enhanced the leaching efficiencies of Cu and Co, while a reduction in particle size (large surface area) favours the leaching of Cu and Co. The highest leaching efficiencies of 99.2 % and 94.0 % were obtained for Cu and Co, respectively, in a leaching system constituted by 1.0 M H_2SO_4 and 3.0 M H_2O_2 within 4 h at 65 °C. In contrast, the 0.8 M OA leaching system demonstrated a 97.1 % efficiency for Cu and 100.0 % efficiency for Co. The estimated activation energy in the temperature range of 25–65 °C is 40.7 $kJmol^{-1}$ for Cu, while that of Co is 64.0 $kJmol^{-1}$, which implies that the leaching is controlled by a surface chemical reaction. A comprehensive analysis demonstrated that the reaction mechanism for Cu leaching is diffusion-controlled at lower temperatures (<35 °C) and surface chemical reaction-controlled at temperatures higher than 35 °C.

1. Introduction

Cu is widely used in industrial machinery and household appliances, while Co serves as a crucial raw material in battery production, alloy formation, catalyst manufacturing, ceramics, and other essential materials (Barman et al., 2023; Lipman and Maier, 2021). So, the recovery of these metals is significantly important. Most of the income in the Democratic Republic of Congo (DRC) comes from the mining industry. The country has some of the richest mineral resources in the world. Mineral resources rich in Cu and Co can be found in the southwest part of this country, which was once the province of Katanga. Approximately 5.0 % of the world's Cu and almost half of its Co are found there (Shengo et al., 2019). In the DRC, several mining companies produce and trade these metals, together holding a notable market share. According to one of these companies, i.e. Glencore's 2021 Annual report, 1.20 million tonnes of Cu and 34,000 tonnes of Co were produced (Crundwell et al., 2020). Sulfide, oxide, and sulfide-oxide mixed ore are the three main categories of Cu–Co ore found in the DRC, and each is handled differently (Crundwell et al., 2020).

Cu exhibits distinctive characteristics, including malleability, as well as exceptional thermal and electrical conductivity. Cu is an essential metal for the world market since it is used in so many applications for daily life, from large industrial machinery to home electrical appliances (Oke et al., 2023). Cu is primarily used in wiring for the production, transmission, and distribution of electricity (Henckens and Worrell, 2020). Cu is a versatile metal because it can be alloyed with a wide variety of other metals (Kundu et al., 2023). Typically, ores containing 0.4–0.8 % Cu are mined for copper (Henckens and Worrell, 2020). Also, Co is a critical raw material, and it has been used extensively in the production of batteries, alloys, catalysts, ceramics, and other materials due to its special qualities, which include ferromagnetism, corrosion resistance, and temperature-dependent crystal structure (Li et al., 2023; Santoro et al., 2019). Perhaps the most well-known application of Co is in lithium-ion batteries as an electrode component. The year 2020 saw

* Corresponding author at: Sustainable and Innovative Minerals and Metals Extraction Technology (SIMMET) Research Group, School of Chemical and Metallurgical Engineering, University of the Witwatersrand Johannesburg, Private Bag X3 PO Wits 2050, Johannesburg, South Africa.
E-mail addresses: emmanuel.oke@wits.ac.za, okeemmanuela@gmail.com (E.A. Oke).

https://doi.org/10.1016/j.mineng.2024.108853
Received 16 April 2024; Received in revised form 15 July 2024; Accepted 16 July 2024
Available online 24 July 2024

the production of batteries consuming 64.0 % of all refined Co in the world (Gulley, 2022). Over 175,000 tons of Co were consumed worldwide in 2021, an increase of about 86.0 % from the 93,950 tons consumed in 2016. Furthermore, by 2050, the demand for Co is predicted to rise significantly (Alvial-Hein et al., 2021).

Sulfide and oxide ores are the two main types of Cu and Co ores. However, the classification of ores may change based on the location and depth of mining. Different approaches to mineral processing, such as pyrometallurgical and hydrometallurgical techniques, are required for these different types of ores (Crundwell et al., 2020; Shengo et al., 2019; Zheng et al., 2023). Because oxide ores can dissolve in aqueous solutions, they are processed through a process called dissolution, whereas sulfide ores are usually treated first by flotation.

Leaching is a crucial step in any hydrometallurgical process and primarily consists of acid or alkali leaching (Raj et al., 2022). Alkali leaching typically involves the leaching of Cu and Al using sodium hydroxide or ammonia, followed by the leaching of Co using reducing acids (Chen et al., 2011). Organic acids like citric acid, ascorbic acid, and oxalic acid, or inorganic acids like sulfuric acid, hydrochloric acid, and nitric acid, are used as leaching agents in acid leaching (Guimarães et al., 2022). Sulfuric acid (H_2SO_4) leaching is frequently used as a practical and adaptable technique for dissolving copper-oxidised ore (Crundwell, 2014; Hosseinzadeh et al., 2021). The leaching of Cu and Co oxide ore is typically categorised into stirring leaching and heap leaching (Schueler et al., 2021). Stirred leaching involves mechanical or air stirring in a diluted H_2SO_4 solution, which is suitable for high-grade Cu ores. On the other hand, heap leaching, which is cost-effective and suitable for low-grade oxidised or waste ores, involves crushing the ore, piling it on a heap, and spraying leaching agents on top to dissolve the Cu. This process is repeated multiple times until satisfactory leaching efficiency is achieved. Co minerals pose a leaching challenge due to their inherent difficulty in leaching without a reductant (Chong et al., 2013). The presence of trivalent Co (Co^{3+}) in both sulfide and oxide minerals results in low solubility in aqueous solutions, leading to a slow leaching rate. To address this issue, a reductant is commonly introduced into the leaching reactors to convert Co^{3+} to the more soluble Co^{2+}. Furthermore, a classic hydrometallurgical method called stirring leaching usually entails dispersing finely ground ore into an acidic solution. It is possible to prevent particle precipitation and enhance leaching kinetics by using a mixing process (Dong et al., 2019).

Organic acids are referred to as “green leaching agents” or “green lixiviants” because they are easily biodegradable and do not emit harmful gases into the environment (He et al., 2017; Li et al., 2018; Mohanty and Devi, 2023). It has been found that organic acids’ metal leaching capacity in some applications is comparable to that of mineral acids (Ozairy et al., 2022). In contrast to inorganic acids like H_2SO_4 and HCl, citric acid as a leaching agent improved the metals’ leaching efficiency in ultrasound-assisted Co leaching (Wang et al., 2020). More than 96.0 % of the Co is leached with 2.0 M citric acid, 0.6 M H_2O_2, 60 °C temperature, 5.0 h leaching time, and 90 W ultrasonic power. Cu and Co were recovered from Cu smelting slag formed at 1350 ^{0}C by leaching and yielded 92.0 % Cu and 95.6 % Co (Li et al., 2017). In a recent study, using an amino acid-based aqueous biphasic system resulted in a leaching efficiency of more than 90.0 % for Cu and Co at a relatively mild temperature of 70 °C and a solid–liquid ratio of 1:10 (Cai et al., 2023).

In the current investigation, H_2SO_4, citric acid (CA), and oxalic acid (OA) in combination with H_2O_2 for the leaching of Cu and Co from a Cu–Co ore. These chemicals were selected based on their strong metal cation binding affinity. In addition, CA and OA were specifically used owing to their high biodegradability and eco-friendliness (Li and Li, 2023; Liu et al., 2022). The primary objective was to investigate the innovative application of H_2SO_4, CA, and OA in leaching processes for extracting Cu and Co from a typical DRC Cu–Co ore. The principal goals include evaluating the efficiency of these acids in enhancing leaching processes and contributing novel insights to the field of hydrometallurgy. Therefore, this study presents a distinctive contribution to optimising metal recovery from complex ores, representing a significant stride in advancing sustainable and environmentally benign mineral processing techniques. This study introduces a pioneering approach by using a combination of CA, OA, and H_2O_2 for the simultaneous leaching of Cu and Co from a Cu–Co ore. This innovative method is being employed for the first time, potentially offering a more efficient and sustainable alternative to traditional leaching techniques.

2. Materials and methods

2.1. Chemicals

Citric acid (CA), oxalic acid (OA), and hydrogen peroxide (H_2O_2) were procured from Associated Chemical Enterprises Pty Ltd, South Africa, while sulfuric acid (H_2SO_4) was provided by Sigma Aldrich. All chemicals were utilised without further purification. The preparation of standard solutions was carried out using deionised water. The structures of the chemicals are illustrated in Fig. 1.

2.2. Sample collection and preparation

The material utilised for this investigation was procured from a commercial company situated in Lualaba, DRC. Initially, the material exhibited rigid agglomerates and underwent comminution, first by using a jaw crusher, followed by a cone crusher. After this, a ball mill operating at 148.0 rpm was employed to further diminish the particle dimensions and disassemble the conglomerates. The resulting finer material underwent an overnight air-drying process to remove any residual moisture. Following this, the dried material was homogenised and classified using standard stainless steel laboratory sieves and an electronic sieve shaker. Specifically, particle sizes (PS) of (−106 + 75) μm, (−75 + 53) μm, and (−53 + 38) μm were chosen to investigate the role of particle size on the leaching efficiency of Cu and Co.

2.3. Sample characterisation

The characterization of the material’s phases was conducted through a multi-faceted approach, combining x-ray diffraction (XRD, Bruker, Karlsruhe, Germany) and scanning electron microscopy with energy dispersive x-ray spectroscopy (SEM-EDX). The XRD analysis revealed pivotal insights into the structural composition, identifying cuprite (Cu_2O) and cobalt oxide (Co_2O_3) as the predominant phases associated with Cu and Co. This information provided a detailed understanding of the crystalline nature of the sample, elucidating the arrangement and orientation of atoms within the material. Complementing the XRD findings, SEM-EDX was employed to examine the morphological features of the sample at a microscale level and simultaneously analyse the elemental composition. Scanning electron microscopy (SEM) facilitated a high-resolution, three-dimensional visualization of the sample’s surface, offering a nuanced exploration of its structural attributes. The concurrent use of energy dispersive x-ray spectroscopy (EDX) allowed for the identification and quantification of elements present in the sample, providing valuable data on the elemental distribution. Additionally, the main chemical composition of the sample was comprehensively characterised using x-ray fluorescence (XRF). This analytical technique enabled the quantitative determination of elemental constituents.

2.4. Leaching tests

For the leaching experiments, closed Schott bottles with a volume of 50.0 mL were employed for each sample. In each experimental trial, 2.0 g of the sample was introduced into a 20.0 mL solution comprising 1.0 M H_2SO_4. These sealed Schott bottles were then placed in a thermostatically controlled shaker, operating at a consistent 500.0 rpm, by varying

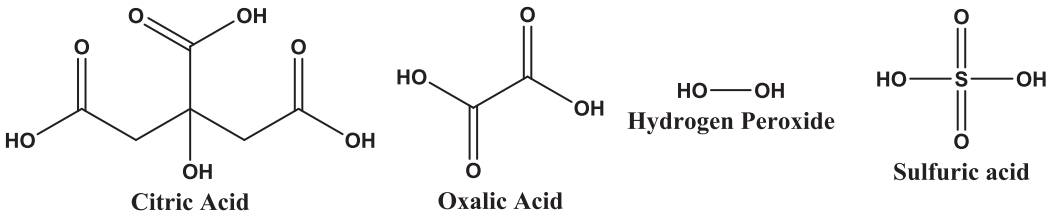

Fig. 1. Structure of the chemicals used in this study.

the temperatures and time from 25 °C to 65 °C and 1.0 h to 8.0 h, respectively. The resulting pregnant solution was subjected to filtration, and the filtrate after appropriate dilution was subsequently analysed using an atomic absorption spectrometer (AAS, Varian AA240, USA) to quantify the extracted amounts of Cu and Co. This provided essential insights into the leaching efficiency of the experimental process. This

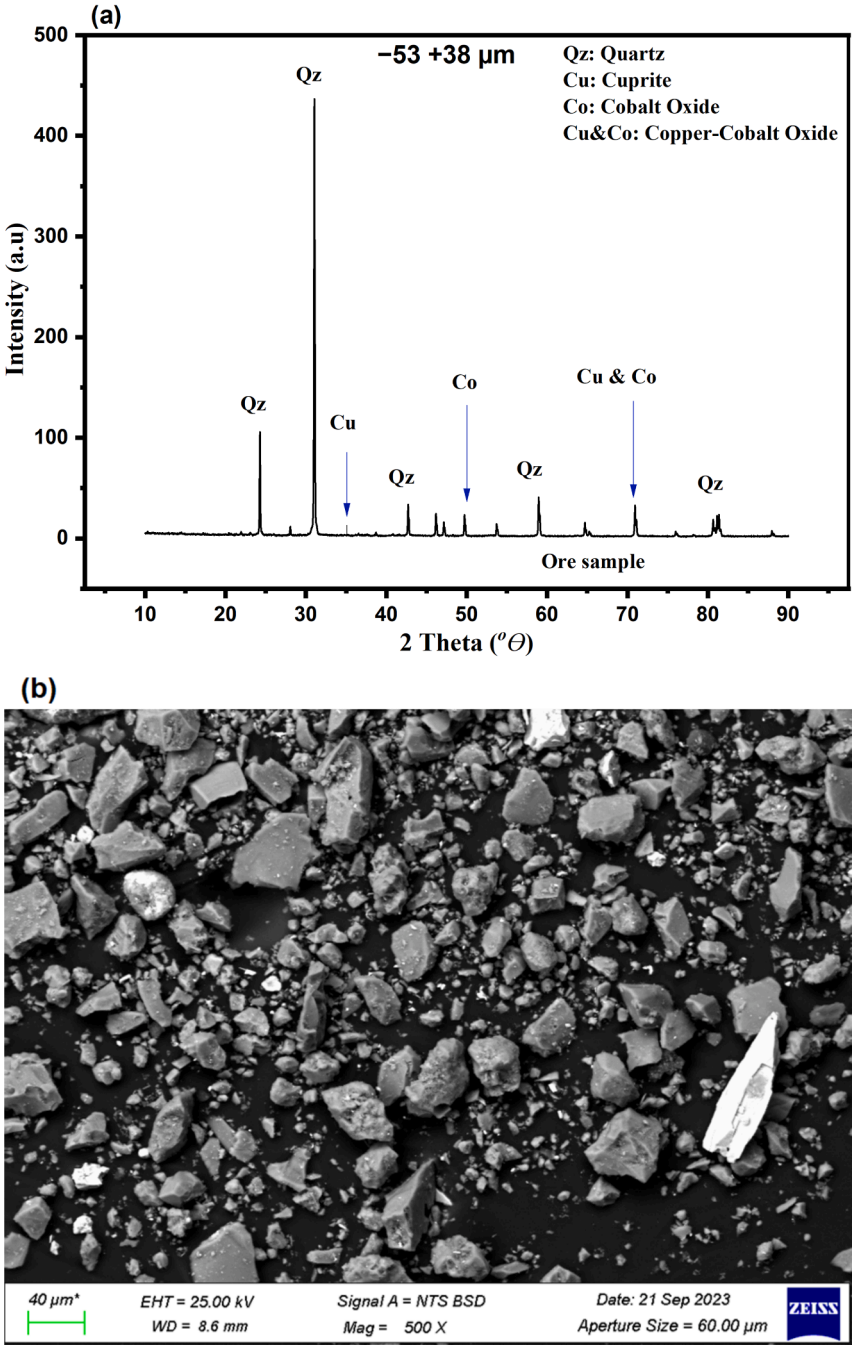

Fig. 2. (a) XRD pattern of the Cu—Co ore with the observed mineral phases; (b) SEM micrograph of the Cu–Co ore before the leaching process; and (c) EDX micrograph of the Cu–Co ore before the leaching test.

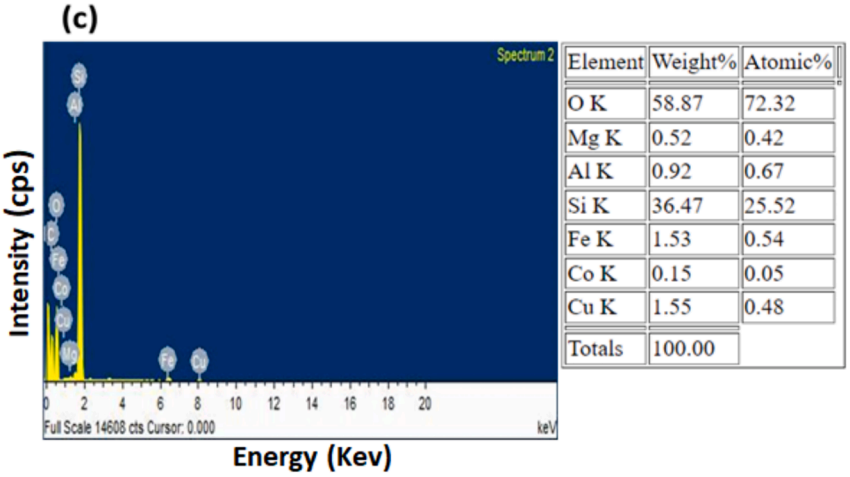

Fig. 2. (*continued*).

procedural approach was consistently applied for other leaching experiments involving the utilisation of CA, OA, and H_2O_2 as an oxidant, ensuring a comprehensive and comparable evaluation of leaching efficiency under different experimental conditions. All experiments were conducted twice to minimise errors and the average values obtained were utilised for the construction of graphs. Good repeatability was observed in all the runs conducted. The leaching efficiency (%) was estimated using equation (I).

$$\text{Leaching Efficiency}\,(\%) = \frac{C_0}{C_i} \times 100 \qquad \text{(I)}$$

in the equation above, C_o denotes the concentration of metal in the filtrate while C_i represents the concentration of metal in the original sample.

3. Results and discussion

3.1. Mineral phase and composition of the Cu-Co ore

The mineralogical analysis of the ore was obtained using XRD. The XRD pattern of the Cu-Co bearing ore with size − 53 + 38 μm is presented in Fig. 2 (**a**). The main phases contained in the material include quartz (SiO_2), cobalt oxide (CoO), cuprite ($Cu_{2+1}O$) and copper-cobalt oxide ($Cu_{0.92}Co_{2.08}O_4$). Also, Fig. 2 **(b & c)** depicts SEM and EDS micrographs and monographs of the Cu-Co ore studied. From the micrographs, the surface looks greyish and smooth with a few defects and pores. In addition, the dark black patches represent Cu and Co oxides. The chemical composition of the Cu-Co ore as revealed by the XRF and XRD data is presented in Table 1 and Table 2**,** respectively. The obtained data indicate that quartz is the predominant component of the sample because it constitutes approximately 93.0–95.0 % of the total mass. The desired metals, Cu and Co are present in relatively lower quantities compared to other metals, with Cu being more abundant than Co. The consistency between the XRF and XRD findings confirms that the Cu–Co ore is mainly oxides.

Table 1
Chemical composition of the investigated Cu–Co ore by XRF.

PS (μm)	Al_2O_3 (Mass %)	Fe_2O_3 (Mass %)	Co_2O_3 (Mass %)	CuO (Mass %)	SiO_2 (Mass %)	Others (Mass %)
−106 + 75	0.95	2.27	0.04	0.66	95.1	0.98
−75 + 53	1.40	2.13	0.07	1.13	94.1	1.17
−53 + 38	1.27	2.33	0.09	1.15	93.5	1.66

Table 2
Chemical composition of the investigated Cu–Co ore by XRD.

XRD PDF Card Number	Mineral Phase	Chemical Formula
00–046-1045	Quartz	SiO_2
00–048-1719	Cobalt Oxide	CoO
00–006-0667	Cuprite	CuO
00–037-0878	Copper Cobalt Oxide	Cu_2CoO_3

3.2. Leaching of Cu and Co

To investigate how metals might leach from the Cu—Co ore, experiments were conducted for the present study. H_2SO_4, CA, and OA were used as lixiviants. Because the current industrial process uses sulphuric acid, the effects of particle size, time, temperature, concentration of acids and H_2O_2 were investigated carefully in a typical industrial concentration of H_2SO_4 acid solution.

3.2.1. Effect of particle size

To investigate the effect of PS on the studied Cu—Co ore, three different PSs comprising − 53 + 38 μm, −75 + 53 μm, and − 106 + 75 μm were chosen as previously mentioned. Investigating the effect of PS in metal leaching experiments is crucial to optimise the reaction kinetics and enhance leaching efficiency for improved metal recovery. Previous findings demonstrate that one of the critical factors influencing the leaching of metal from a solid is particle size (Olaoluwa et al., 2023; Zhang et al., 2018). As shown in Fig. 3, we observed that the sample with the smallest PS (−53 + 38 μm) displayed the best leaching efficiencies of 61.3 % and 14.7 % for Cu and Co, respectively. On the other hand, the sample with the PS of − 106 + 75 μm (the largest PS) resulted in the lowest leaching efficiencies of 48.4 % and 10.0 % for Cu and Co, respectively. In other words, the effect of PS on the leaching of Cu and Co follows the trend − 106 + 75 μm (Cu = 48.4 %; Co = 10.0 %) < − 75 + 53 μm (Cu = 55.7 %; Co = 12.5 %) < − 53 + 38 μm (Cu = 61.3 %; Co = 14.7 %). This can be ascribed to the fact that a larger surface area for interaction with the leaching agent is typically provided by smaller particle sizes, which may result in more effective metal recovery. This is because the metals within the particles are more accessible to the leaching solvent. In their studies, Mohanraj et al. and Xu et al. both also explore the role of particle size on metal leaching efficiency (Mohanraj et al., 2022; Xu et al., 2023). Moharang et al. focused on Cu recovery from a Cu ore using a 5 M H_2SO_4 solution at a constant speed of 300 rpm for 30 min. They found that finer particle sizes (−75 + 63 μm and − 63 + 53 μm) achieved the highest Cu leaching efficiencies of approximately

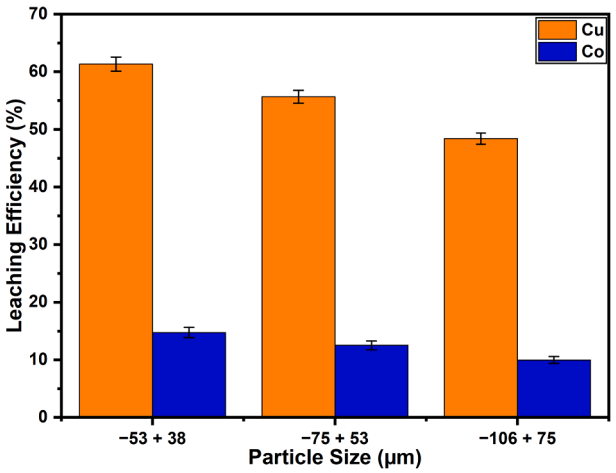

Fig. 3. Effect of particle size on Cu and Co leaching (experimental conditions: H_2SO_4 = 1.0 M; T=25 °C; t = 4.0 h; S/L=1:10; and stirring speed = 500.0 rpm).

28.98 % and 28.50 %, respectively while the larger particle sizes (i.e. − 600 + 355, −355 + 180, −180 + 150, −150 + 125, −125 + 90, and − 90 + 75) resulted in lower leaching efficiencies. They noted that smaller particle diameters increase surface area exposure, enhancing the leaching efficiency, although sizes below − 53 μm led to slime formation that hindered copper dissolution. Similarly, Xu et al. examined Co leaching, observing that reducing particle size from 0.15 mm to 0.10 mm in Cu-Co ore increased Co recovery from 38.6 % to 44.2 %, attributing this improvement to greater acid interaction surface area in finer particles, thereby enhancing Co leaching effectiveness. Since our results demonstrated the best leaching efficiencies for both Cu and Co when the sample with − 53 + 38 μm PS was leached, it was selected for further investigation.

3.2.2. *Effect of time and temperature*

From a process economics standpoint, time and temperature are important considerations. The process's economics will be enhanced by the increased process efficiency brought about by the optimised time and temperature conditions. Thus, to examine their roles in the leaching of Cu and Co, the leaching time and temperature were adjusted from 1.0 h to 8.0 h and 25 °C to 65 °C, respectively. The findings depicted in Fig. 4 (**a & b**) show that time and temperature have a significant impact on the leaching of Cu and Co. For instance, the leaching efficiencies of Cu and Co were 56.9 %, and 13.1 %, respectively, at 25 °C and 1.0 h leaching time. Interestingly, when the leaching time was adjusted to 6.0 h at 25 °C, there was an improvement in the leaching efficiencies to 62.7 % and 24.1 % for Cu and Co leached, respectively. The enhancement in leaching efficiencies for Cu and Co, observed while extending the leaching time from 1.0 h to 8.0 h at 25 °C, can be ascribed to the prolonged duration facilitating more interaction between the leaching solution and the solid material. The extended timeframe allows the leaching agents to penetrate and react more with the mineral surfaces, resulting in a more thorough extraction of both Cu and Co from the sample, consequently yielding higher leaching efficiencies. However, when the leaching duration was raised beyond 6 h, no significant changes were observed in the leaching efficiencies of both Cu and Co. In other words, 6.0 h was observed as the optimal time for leaching the selected metals. Similar observations were reported by Wu et al. in which methanesulfonic acid in combination with H_2O_2 was employed for leaching of Cu from chalcopyrite (Wu et al., 2021). To assess the role of temperature on the leaching of Cu and Co, a range of 25 °C to 65 °C was used as previously posited. An increase in temperature was found to be favourable for the leaching of the studied metals. For example, the lowest leaching efficiencies of Cu and Co were 62.7 % and 15.3 %, respectively, at 25 °C after a 6.0 h leaching duration. Interestingly, after 6.0 h of leaching at 65 °C, the leaching efficiencies of Cu (98.7 %) and Co (72.8 %) significantly improved, as can be seen in Fig. 4 (**a & b**). Enhanced reaction kinetics at higher temperatures are responsible for the higher leaching efficiencies observed at higher temperatures. Higher temperatures cause molecules to collide more frequently, which raises the reaction rate and increases the amount of metal leached (Oke and Potgieter, 2024; Preetam et al., 2022; Salem, 2023).

3.2.3. *Effect of H_2O_2 oxidant*

H_2O_2 is crucial in metal leaching as it serves as a potent oxidising agent, facilitating the dissolution of metals into solution and enhancing leaching rates. Its versatility, environmental friendliness, and ability to provide controlled reaction conditions make it an important component in optimising metal extraction processes. Therefore, in this study, the effect of the concentration of H_2O_2 ranging from 1.0 M to 4.0 M on the leaching of Cu and Co from the ore was investigated. As can be seen in Fig. 5, the introduction of H_2O_2 increases the leaching of Cu and Co significantly. About 69.2 % of Co could be leached in the absence of H_2O_2, whereas approximately 95.1 % of Cu could be leached in its presence. In addition, the introduction of 1.0 M H_2O_2 into the leaching solution did not have any significant effect on the leaching of both metals. However, the addition of 2.0 M H_2O_2 significantly increased the leaching efficiency of Co from 69.2 % to 85.6 %, although its effect on the leaching of Cu was less dramatic (97.3 %). Furthermore, maximum

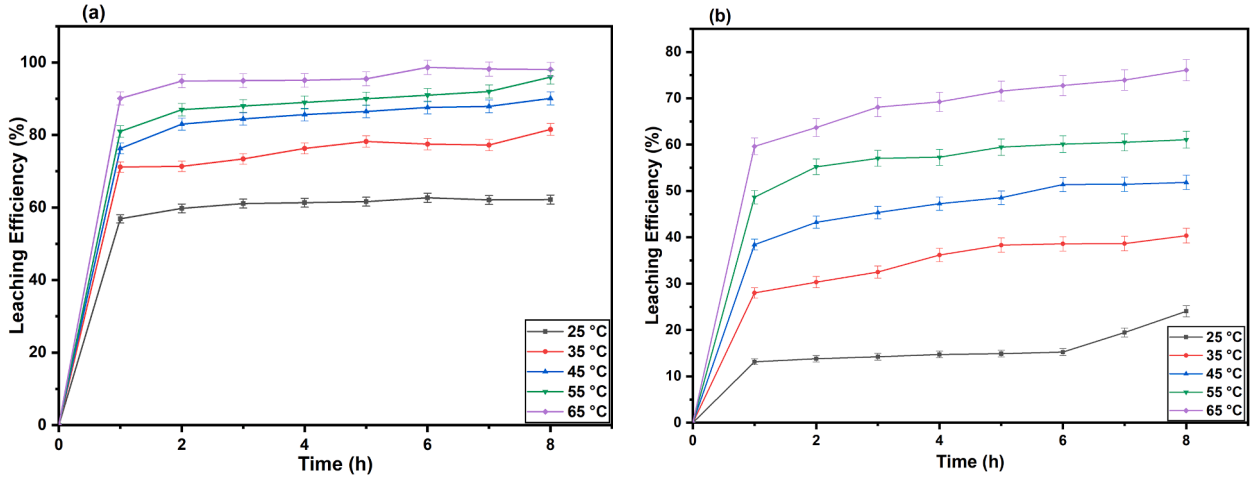

Fig. 4. (a) Effect of time and temperature on leaching of Cu; (b) Effect of time and temperature on leaching of Co (experimental conditions: H_2SO_4 = 1.0 M; T=25 − 65 °C; t = 1.0 − 8.0 h; S/L ratio = 1:10; and stirring speed = 500.0 rpm).

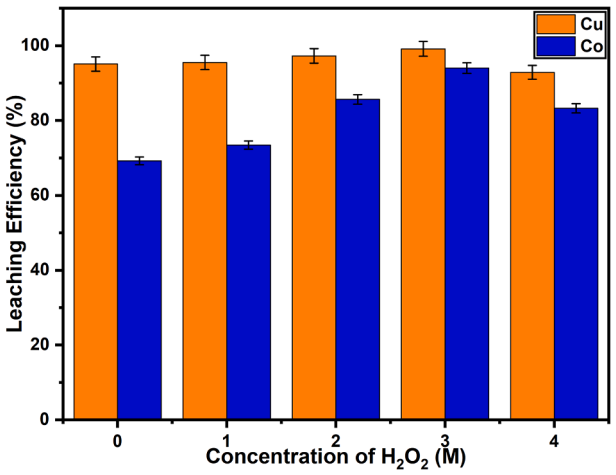

Fig. 5. Effect of H_2O_2 concentration on Cu and Co leaching (experimental conditions: H_2SO_4 = 1.0 M; T=65 °C; t = 4.0 h; S/L=1:10; and stirring speed = 500.0 rpm).

leaching efficiencies of 99.2 % and 94.0 % were achieved for Cu and Co, respectively, at 3.0 M H_2O_2. These results demonstrate a significant improvement in the leaching of Co. However, when the concentration of H_2O_2 increased beyond 3.0 M, the leaching efficiencies of Cu and Co tend to decline significantly. In other words, the optimum leaching for both metals was reached at 3.0 M H_2O_2. A similar observation was reported by Stuurman et al. in their study involving comparing the extent of dissolution of a Cu—Co ore (Stuurman et al., 2014).

Furthermore, to leach metals, O_2 must be present in the acidic solution and H_2O_2 is a useful source of dissolved O_2 in the leaching system because of its potent oxidising power (Wang et al., 2016). Equations (II)–(IV) illustrate how dissolved O_2 is generated as a result of H_2O_2 breakdown (Li et al., 2020). The metal–acid complex is formed when the dissolved O_2 combines with the metals to produce metal oxides. Metal leaching is aided by the high standard reduction potential of 2.4 V that is induced by the OH^- radicals in the leaching solution (Jadhao et al., 2021).

$$H_2O_{2(aq)} + 2e^- \rightarrow 2OH^-_{(aq)} \quad \text{(II)}$$

$$H_2O_{2(aq)} + e^- \rightarrow OH^-_{(aq)} + OH^-_{(aq)} \quad \text{(III)}$$

$$2H_2O_{2(aq)} \rightarrow 2H_2O_{(l)} + O_{2(g)} \quad \text{(IV)}$$

3.3. Effect of different concentrations of organic acids

In this study, organic acids, specifically CA and OA, were employed to investigate the leaching of the metals of interest. Although CA and OA are weak acids, they are excellent chelating agents and metal binders. They aid mineral dissolution by specifically adsorbing on mineral surfaces and forming highly soluble complexes with metal ions. The formation of ligand–metal complexes at the mineral surface shifts the electron density toward the metal ions (Astuti et al., 2016). In general, as the concentration of the leaching agent rises, so does the metal recovery (Nagarajan and Panchatcharam, 2023).

In this study, the concentrations of CA and OA were varied from 0.4 M to 1.0 M and 2.0 M H_2O_2 was added during the leaching process. It was found that the leaching efficiencies of Cu and Co increased as the concentration of the organic leaching agents increased and began to reduce at higher concentrations, as depicted in Fig. 6 **a & b**. For instance, when the leaching process was carried out with 0.4 M CA, the leaching efficiencies of Cu and Co were respectively 65.7 % and 84.6 %. However, optimum leaching efficiencies of 88.7 % and 99.9 % were obtained for Cu and Co respectively when the concentration of CA was increased to 0.6 M. However, when the concentration of CA was further increased, the leaching efficiencies of both metals started to decrease (Fig. 6a). A similar trend was observed when OA was applied for the leaching process. In fact, when the OA concentration was increased to 0.8 M, complete leaching of Co (100.0 %) and 97.1 % of Cu was noticed beyond which the leaching efficiency declined (Fig. 6b). This is because metals combined with citrate/oxalate to form complexes, which are then broken down by H_2O_2 to release free metal ions into the solution. Leaching efficiency decreases as concentration rises because the acids form more complexes with the metals but cannot convert them to metal ions because there is insufficient H_2O_2 (Nagarajan and Panchatcharam, 2023).

In addition, both organic acids used in this study demonstrated better leaching efficiencies for Co compared to Cu. For example, the leaching system constituted by 0.6 M CA led to 88.7 % (Cu) and 99.9 % (Co) leaching efficiencies (Fig. 6a). Also, 0.8 M OA leaching system demonstrated 97.1 % efficiency for Cu and 100.0 % efficiency for Co leaching (Fig. 6b). The strong affinity of CA and OA for Co likely contributes to their better leaching efficiencies for Co compared to Cu under the same experimental conditions. In addition, leaching systems composed of OA displayed higher leaching efficiencies for both Cu and Co compared to leaching systems constituted by CA under the same experimental

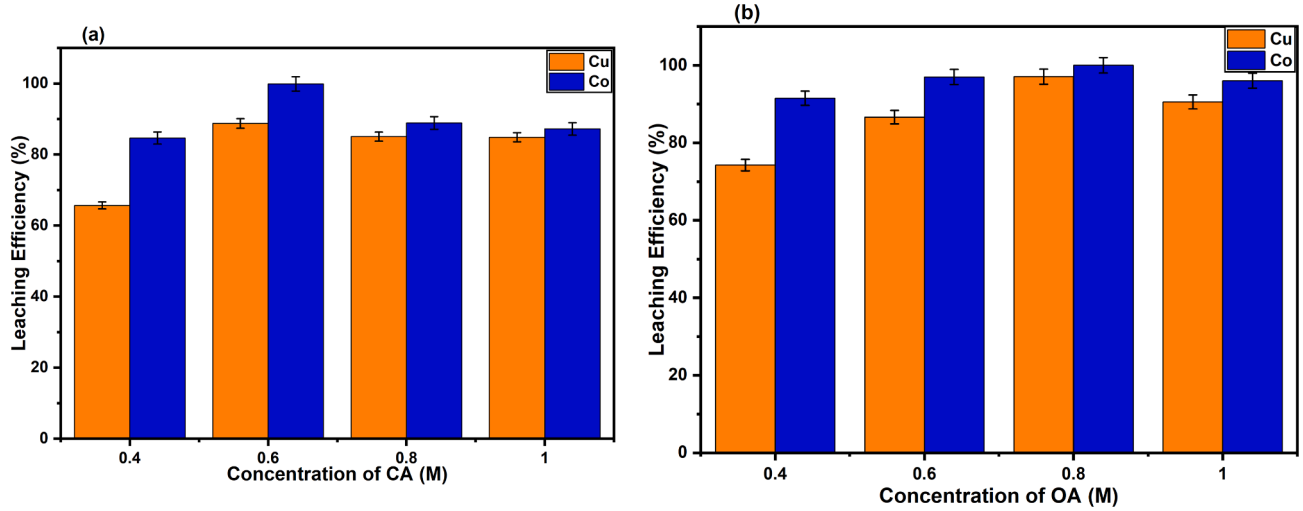

Fig. 6. Effect of (a) CA concentrations; (b) OA on Cu and Co leaching (experimental conditions: H_2O_2 = 2.0 M; T=65 °C; t = 4.0 h; S/L ratio = 1:10; stirring speed = 500.0 rpm).

conditions in most cases. For example, when 0.80 M of both CA and OA was applied for the leaching process, for the leaching platform constituted by CA, 85.0 % Cu was leached whereas the OA system resulted in 97.1 % Cu recovery. A similar trend was observed for the leaching of Co. This behaviour can be attributed to the fact that CA has higher dissociation constants and lower ionisation constants compared to OA (Xu et al., 2019). This implies that OA is a stronger acid and can more easily form complexes with metal ions compared to CA.

Also, in the proton-promoted dissolving process, H^+ is produced as an organic acid dissociates. Organic acids can dissolve metals by supplying ligands and protons. Equations (V)–(VII) show how they can dissolve the metallic components in the sample by forming complexes and acidifying them (Nagarajan and Panchatcharam, 2023).

$$RCOOH + H_2O \leftrightarrow RCOO^- + H_3O^+ \quad (V)$$

Proton reduction produces hydrogen and oxidizes the metal,

$$2H_3O^+ + 2e^- \rightarrow H_2 + 2H_2O \quad (VI)$$

$$M\ (metal) \rightarrow M^{2+} + 2e^- \quad (VII)$$

In a complexation mechanism, the ligands in organic acids, such as citrate from citric acid and oxalate from oxalic acid, produce stable metal complexes. The complexation reaction, shown in equation (VIII), shifts the equilibrium to the right and causes metals to dissolve more easily in solutions (Steer and Griffiths, 2013).

$$RCOO^- + M\ (H_3O^+) \rightarrow RCOOM + H_2O \quad (VIII)$$

Another potential mechanism is that in the presence of H_2O_2, citric acid, and oxalic acid, metals from the sample investigated could react to form metal hydrogen citrate/oxalate, as shown in equation (IX).

$$C_6H_8O_7\ (CA) / C_2H_2O_4\ (OA) + M + H_2O_2 \rightarrow M\ (C_6H_8O_7) / M\ (C_2H_2O_4) + H_2O + M^{2+} \quad (IX)$$

3.4. Analysis of Residue

The residue obtained after leaching Cu and Co (experimental conditions: OA=0.8 M; H_2O_2 = 2.0 M; T=65 °C; t = 4.0 h; S/L ratio = 1:10; stirring speed = 500.0 rpm) from the investigated Cu-Co ore was analysed by SEM, EDS and XRD as shown in Fig. 7 **a-c**, respectively. In addition, XRF was used to complement the previously mentioned and

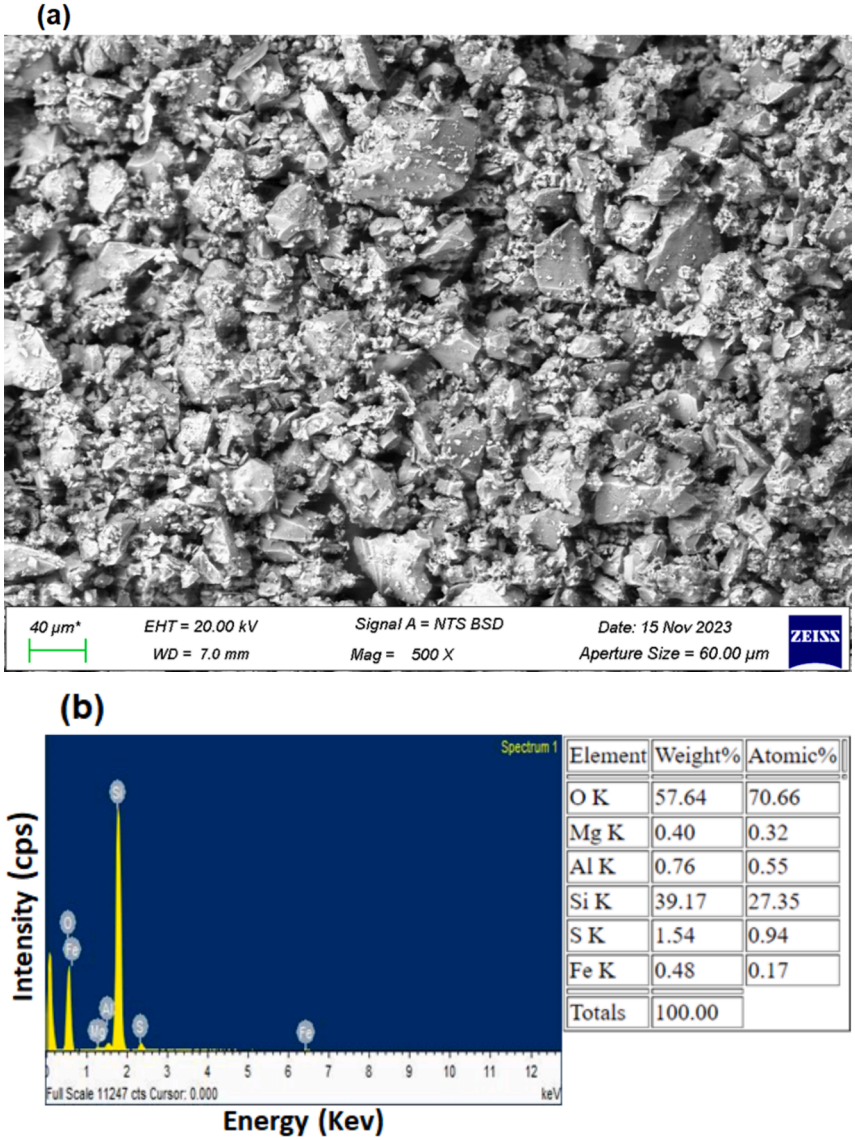

Fig. 7. (a) SEM; (b) EDS results of Cu-Co ore after the leaching process; and (c) XRD patterns before and after the leaching process.

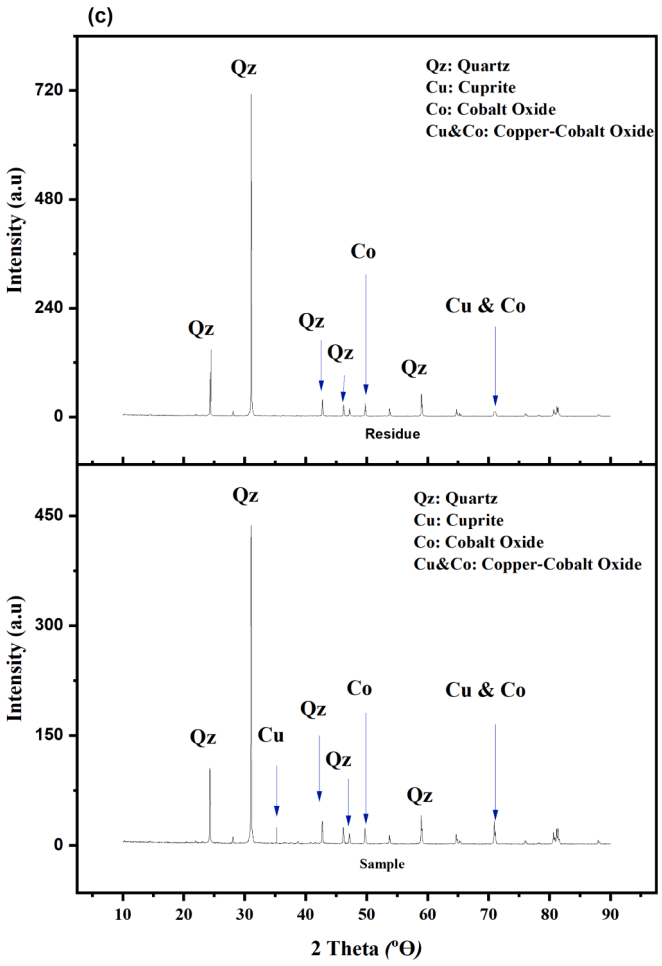

Fig. 7. (*continued*).

the results obtained are presented in Table 3. These analyses were carried out on the residue of the sample to prove that almost complete leaching of Cu and Co truly occurred using 0.8 M OA. Fig. 2b illustrates the image for the SEM analysis of the investigated sample before leaching. This sample contained a layer of Cu and Co on its surface as clearly shown by the SEM image. Significant inputs and confirmations for the leaching process usually come from the morphology, chemical composition, and characterisation of the residue following the leaching process. The leached residue's morphology (Fig. 7a) reveals that it is porous and corroded. Pits on the sample represent areas of the surface that have been leached successfully. The EDS results show the absence of Cu and Co (Fig. 7b) which can also be observed by the SEM image resembling that of silica as shown in Fig. 7a. The O and Si content are 57.6 % and 39.2 %, respectively, while the remaining are made up by Mg, Al, S, and Fe. Furthermore, Fig. 7c shows the mineral phases of the original sample against the leached residue using XRD. In this case, a decrease in the peak intensity of the phases at $2\theta = 36.47^{\circ}$ and 49.23°, which correspond to the targeted metals (Cu and Co), was observed in the leached residue. Additionally, an increase in gangue-related minerals, such as quartz, was identified in the solid residue. The decrease in peak intensity suggests mineral phase dissolution, while the increase in gangue-related mineral intensity could be attributed to the enrichment caused by the withdrawal of the targeted metals. XRF analysis of the residue (Table 3) also demonstrated that the residual product undergoes a quantitative transformation.

Table 3
Chemical composition of the residual product after leaching by XRF.

Chemical Composition (Mass %)	Al_2O_3	Fe_2O_3	Co_2O_3	CuO	SiO_2	Others
Residue	1.20	1.66	0.001	0.05	95.94	1.15

3.5. Leaching kinetics

Because the current industrial process utilises sulphuric acid leaching, it was decided to investigate the leaching process of the H_2SO_4—H_2O_2 system in further detail. In order to investigate the kinetics of ore dissolution, it was assumed that the ore particles were non-porous, spherical particles. This means that the initial reaction takes place on the particle surface, leading to the formation of a solid product layer on the ore surface. Thus, the leaching agent (H_2SO_4) first moves through the product layer and then proceeds to react at the interface where the solid product layer and the unreacted solid phase meet (Olaoluwa et al., 2023). In other words, the reaction between solid and liquid that occurs during the leaching of the Cu–Co ore particles is determined by the diffusion rate as well as the interfacial chemical reaction (Li et al., 2024). While retaining the non-metallic components, the leaching solution dissolves the metallic Cu—Co from the ore's surface. The reaction zone gradually expands inward while the metal particle surface contracts during the reaction process. Thus, the leaching kinetics based on the shrinking core model (SCM) was used to analyse the leaching process of metallic Cu—Co in the ore for leaching temperatures ranging from 25 °C to 65 °C and leaching times between 1.0 h and 8.0 h (other experimental conditions: H_2SO_4 = 1.0 M; S/L ratio = 1:10; and stirring speed = 500.0 rpm) to clarify the leaching mechanism

of Cu–Co ore. The surface chemical reaction model equation (X), internal diffusion equation (XI), and the mixed control model equation (XII) make up the conventional SCM leaching model. Schematic representation of the experimental results using these equations (X)–(XII), is one of the methods of identifying what governs the reaction rate. The fitted model is represented by a linear relationship between the reaction time and the left side of any of the following equations (Teimouri et al., 2020):

$$1-(1-X)^{1/3} = k_1 t \quad (X)$$

$$1-3(1-X)^{2/3}+2(1-X) = k_2 t \quad (XI)$$

$$1/3\ln(1-X)+[(1-X)^{-1/3}-1] = k_3 t \quad (XII)$$

in the above equations, X represents the fraction of Cu—Co leached at any given time (t), while k_1, k_2, and k_3 denote the rate constants associated with chemical reaction, diffusion, and mixed control, respectively.

The SCM graphs for Cu are shown in Fig. 8 (**a–c**), with their corresponding R^2 values at different temperatures presented in Table 4. Also, the SCM graphs for Co are depicted in Fig. 9 (**a–c**) with their R^2 values shown in Table 5. The leaching process of metallic Cu in the Cu—Co ore conforms mostly with the diffusion model. In other words, equation (XI) has a better linear fitting relationship with the experimental kinetic data in which the obtained R^2 values ranged between 0.723 and 0.969 (Table 4). On the other hand, the R^2 values obtained for Cu when equations (X) and (XII) were applied for modelling of the experimental data, varied between 0.716 and 0.877 and 0.651–0.964, respectively. Therefore, it can be deduced that the leaching of Cu from Cu–Co ore is a dissolution process controlled by diffusion. Furthermore, the fitting results show that the dissolution process of metallic Co is mainly a mixed control process, with equations (X)–(XII) having linear regression fit coefficients of R^2 between 0.714 and 0.962, 0.662–0.971, and 0.651–0.986, respectively (Table 5). The experimental data therefore did not fit equations (X) and (XI) very well. Overall, the leaching of Cu is a diffusion-dominated process, while that of Co is a mixed-controlled process.

Table 4
SCM fitting equations for Cu leaching at varying temperatures.

Limiting Step	SCM Model Equation	R^2 @ 25 °C	R^2 @ 35 °C	R^2 @ 45 °C	R^2 @ 55 °C	R^2 @ 65 °C
Chemical reaction control	$1-(1-X)^{1/3} = k_1 t$	0.716	0.878	0.888	0.886	0.877
Diffusion control	$1-3(1-X)^{2/3}+2(1-X) = k_2 t$	0.723	0.879	0.936	0.956	0.969
Mixed control	$1/3\ln(1-X)+[(1-X)^{-1/3}-1] = k_3 t$	0.651	0.877	0.959	0.888	0.964

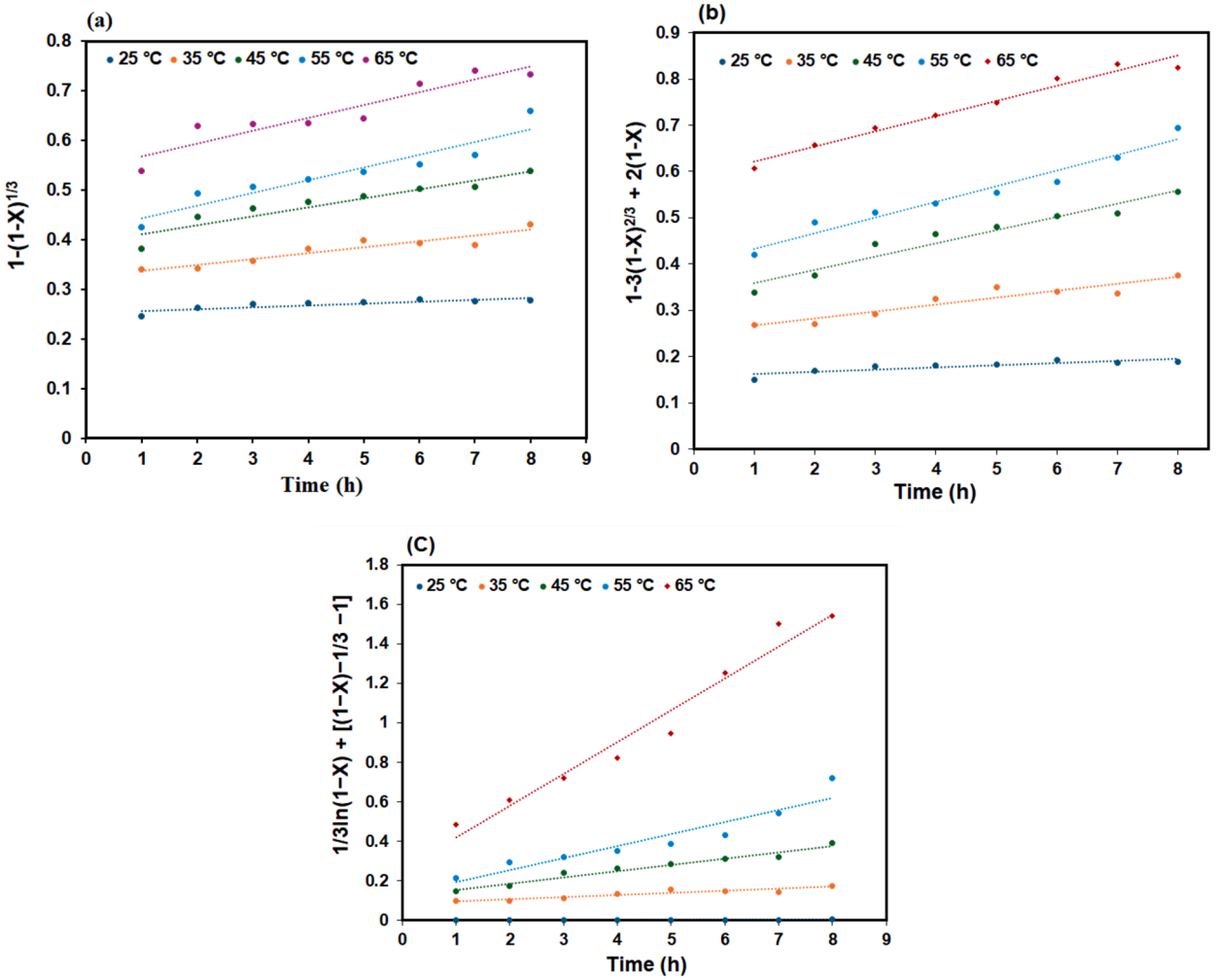

Fig. 8. SCM graphs for Cu leaching at different temperatures: (a) chemical reaction control; (b) diffusion control; and (c) mixed control (experimental conditions: H_2SO_4 = 1.0 M; T=25 − 65 °C; t = 1.0 − 8.0 h; S/L ratio = 1:10; and stirring speed = 500.0 rpm).

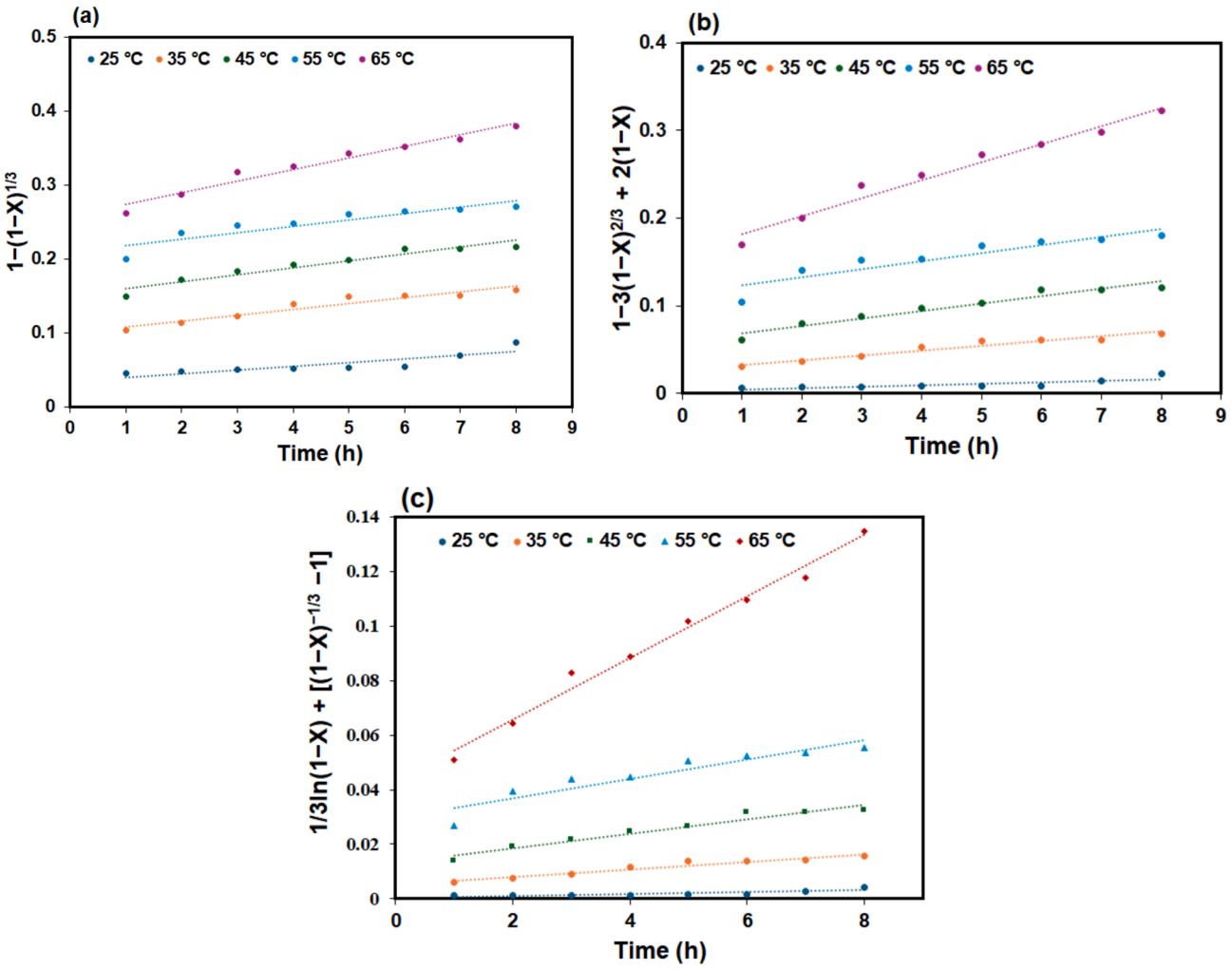

Fig. 9. SCM graphs for Co leaching at different temperatures: (a) chemical reaction control; (b) diffusion control; and (c) mixed control (experimental conditions: H_2SO_4 = 1.0 M; T=25 − 65 °C; t = 1.0 − 8.0 h; S/L ratio = 1:10; and stirring speed = 500.0 rpm).

Table 5
SCM fitting equations for Co leaching at varying temperatures.

Limiting Step	SCM Model Equation	R^2 @ 25 °C	R^2 @ 35 °C	R^2 @ 45 °C	R^2 @ 55 °C	R^2 @ 65 °C
Chemical reaction control	$1-(1-X)^{1/3} = k_1t$	0.714	0.921	0.925	0.818	0.962
Diffusion control	$1-3(1-X)^{2/3}+2(1-X) = k_2t$	0.662	0.933	0.941	0.841	0.971
Mixed control	$1/3\ln(1-X) + [(1-X)^{-1/3} - 1] = k_3t$	0.651	0.938	0.951	0.869	0.984

3.6. Activation energy estimation for the leaching process

The rate-controlling step of a reaction depends on the activation energy required, which can be a significant factor in the process. In this case, the correlation between the reaction rate constant (k) and temperature for various kinetic models is described by Arrhenius' law, which can be applied to estimate the activation energy of the leaching process. The Arrhenius' equation is presented in equation (XIII) below:

$$k = Ae^{-Ea/RT} \quad \text{(XIII)}$$

in the equation above, k is the constant of reaction (h^{-1}), *A* is the frequency factor, *Ea* is the apparent activation energy of the leaching process ($kJmol^{-1}$), *R* is the universal gas constant (8.314 $Jmol^{-1}K^{-1}$), and *T* is the absolute temperature (K).

To find the activation energy for Cu and Co, the slopes of the straight lines in Fig. 8 and Fig. 9 were utilised to estimate the "k". Fig. 10 (**a**–**c**) shows the graphs of the natural logarithm of the apparent rate constant (ln k) against the inverse of the corresponding temperatures (1/T) using equation (XIII) for the investigated metals.

The magnitude of the activation energy can assist in predicting the type of leaching process mechanism. A leaching process that is controlled by diffusion is typically indicated by a value less than 40.0 $kJmol^{-1}$, while one that is controlled by a chemical reaction is indicated by a value greater than 40.0 $kJmol^{-1}$ (Olaoluwa et al., 2023; Salem, 2023). The data in Fig. 10a indicated that the activation energy for Cu leaching was 40.7 $kJmol^{-1}$ (not significantly greater than 40.0 $kJmol^{-1}$) over the entire temperature range (25 − 65 °C), demonstrating that diffusion controls the leaching of the Cu metal. This observation further supports the R^2 fitting obtained for Cu using equation (XI) of the SCM as previously described. In addition, the temperature range was split into two regimes for a more thorough analysis: 25–35 °C and 35–65 °C. As illustrated in Fig. 10b, the activation energy was determined to be 2.8 $kJmol^{-1}$ between 25 °C and 35 °C and 71.4 $kJmol^{-1}$ between 35 °C and 65 °C. The outcome suggests that diffusion governs the reaction mechanism at lower temperature regimes through the product layer. It changed to a controlled surface chemical reaction in the higher

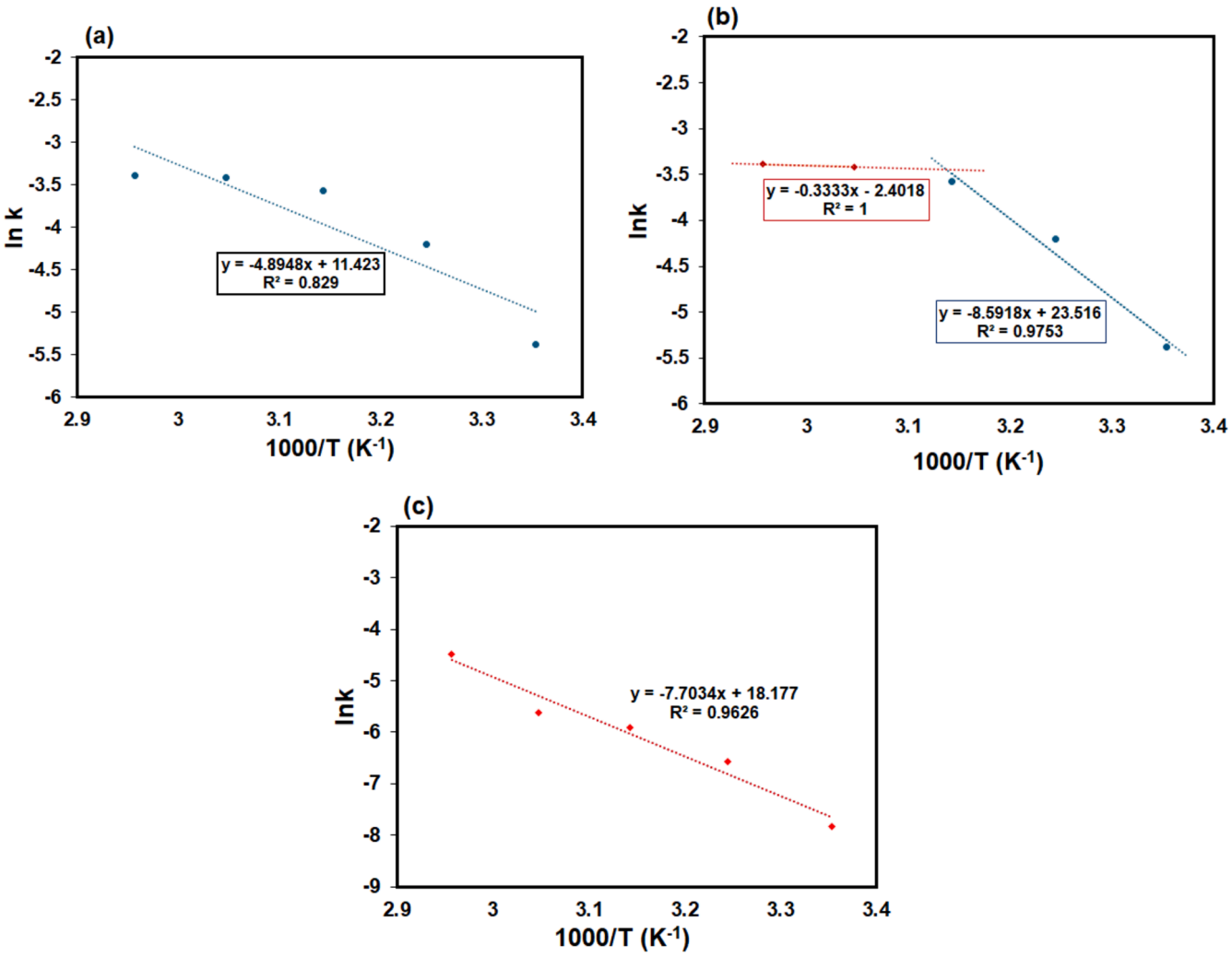

Fig. 10. Arrhenius plots for the leached metals using H_2SO_4–H_2O_2: (a) fitting over the whole temperature range for Cu; (b) fitting for two temperature regimes for Cu; and (c) fitting in the whole temperature range for Co.

temperature range. In a recent study by Wu et al. on the leaching of Cu from chalcopyrite concentrate using methanesulfonic acid (MSA) and H_2O_2 at various temperatures, similar observations were reported (Wu et al., 2021). Furthermore, in this study, the activation energy for the leaching of Co was estimated to be 64.0 kJmol^{-1} (Fig. 10c). Since the activation energy obtained for the Co leaching process is greater than 40 kJmol^{-1}, it can be concluded that the leaching of Co from Cu—Co using the H_2SO_4—H_2O_2 leaching system is controlled by surface chemical reaction over the temperature range investigated. An investigation by Nasab et al. in which Co was leached from iron-rich laterite ore using H_2SO_4 acid at atmospheric pressure similarly suggested that the leaching process for Co is governed by surface chemical reaction (Hosseini Nasab et al., 2020). A more comprehensive comparison between our study and those in the literature is presented in Table 6.

4. Conclusions

The leaching of Cu and Co from Cu-Co ore was investigated using H_2SO_4—H_2O_2, CA—H_2O_2 and OA—H_2O_2 leaching platforms. Our results displayed the best leaching for both Cu and Co (Cu = 61.3 %; Co = 14.7 %) when the sample with − 53 + 38 μm particle size was leached using 1.0 M H_2SO_4 at 25 ^{0}C without H_2O_2. For Cu and Co, respectively, the highest leaching efficiencies of 99.2 % and 94.0 % were achieved in 4 h at 65 ℃ using a leaching system consisting of 1.0 M H_2SO_4 and 3.0 M H_2O_2. Also, maximum leaching efficiencies of 88.7 % and 99.9 % were obtained for Cu and Co respectively when the concentration of CA was raised to 0.6 M. Furthermore, when the OA concentration was increased to 0.8 M, complete leaching of Co (100.0 %) and 97.1 % of Cu was leached. In addition, under the same experimental conditions, leaching with OA typically showed higher leaching efficiencies for both Cu and Co than with CA. This behaviour was explained by the fact that, in comparison to OA, CA has lower ionization constants, and their metal complexes have higher dissociation constants. Comparing the leaching performance of H_2SO_4 and organic acids, it was noted that organic acids also exhibited outstanding results for Cu and Co. For instance, under similar experimental conditions, leaching systems H_2SO_4—H_2O_2, CA—H_2O_2 and CA—H_2O_2 respectively demonstrated (Cu = 97.3 %, Co = 69.2 %), (Cu = 84.8 %, Co = 87.2 %), and (Cu = 90.6 %, Co = 96.0 %). It seemed that the sulphuric acid-hydrogen peroxide combination is best for Cu leaching, while the organic acids-hydrogen peroxide combinations produced higher Co yields. This may indicate a possible route for sequential leaching of Cu and Co from the ore, and it warrants further investigation. The SCM analysis showed that the leaching of Cu is governed by internal diffusion while that of Co is a mixed controlled process when leached with H_2SO_4—H_2O_2 in temperatures ranging from 25 °C to 65 °C. The activation energy for Cu over the range 25–65 °C is 40.7 kJ/mol indicating that Cu leaching is diffusion-controlled. On the other hand, the activation energy of Co is 64.0 kJ/mol, indicating surface chemical reaction control for Co leaching. Because of the high leaching yields obtained with the two organic acids in this investigation, further

Table 6
Comparison between our results of Cu-Co ore leaching using H_2SO_4–H_2O_2 with the literature.

Nature of the Sample	Metals	Experimental Conditions	Leaching Kinetics	Activation Energy ($kJmol^{-1}$)	Leaching Efficiency (%)	References
Copper oxide ore	Cu	H_2SO_4 = 0.77 M; PS=80 %–62.23 μm; S/L=13 %, t = 1.0 h; stirring speed = 500 rpm; & T=70 °C	Mixed control	24.0	97.0	(Clotilde Apua and Madiba, 2021)
Copper oxide	Co	H_2SO_4 = 0.77 M; PS=80 %–62.23 μm; S/L=13 %, t = 1.0 h; stirring speed = 500 rpm; & T=70 °C	Mixed control	28.1	85.4	(Clotilde Apua and Madiba, 2021)
Cobalt-rich copper sulfide ore	Cu	H_2SO_4 = 100 g/L; S/L=0.25 g/mL; t = 4.0 h; & T=60 °C	–	–	95.9	(Yang et al., 2023)
Cobalt-rich copper sulfide ore	Co	H_2SO_4 = 100 g/L; S/L=0.25 g/mL; t = 4.0 h; & T=60 °C	–	–	86.2	(Yang et al., 2023)
Copper-cobalt oxide ore	Cu	H_2SO_4 = 178 kg/t; PS=0.1; slurry density = 33.0 %; & reductant = 100 kg/t	–	–	88.4	(Xu et al., 2023)
Copper-cobalt oxide ore	Co	H_2SO_4 = 178 kg/t; PS=0.1; slurry density = 33.0 %; & reductant = 100 kg/t	–	–	74.6	(Xu et al., 2023)
Iron-rich laterite ore	Co	H_2SO_4 = 5.0 M; S/L=0.1, t = 2.0 h; stirring speed = 370 rpm; & T=90 °C	Chemical control	45.7	63.1	(Hosseini Nasab et al., 2020)
Chalcopyrite	Cu	MSA=30.0 g/L; H_2O_2 = 0.9 vol%; PS=40 μm; S/L=0.01, t = 72.0 h; stirring speed = 370 rpm; & T=70 °C	(a) Diffusion control (for 25–55 °C). (b) Chemical control (55–75 °C)	(a) 22.6 (for 25–55 °C) (b) 148.2 (55–75 °C)	99.0	(Wu et al., 2021)
Copper-cobalt ore	Cu	H_2SO_4 = 1.0 M; PS= − 53 + 38 μm; H_2O_2 = 3.0 M; S/L=0.1 t = 4.0 h; stirring speed = 500 rpm; & T=65 °C	(a) Diffusion control (for 25–35 °C). (b) Chemical control (35–65 °C)	(a) 2.8 (for 25–35 °C) (b)71.4 (35–65 °C)	99.2	This study
Copper-cobalt ore	Co	H_2SO_4 = 1.0 M; PS= − 53 + 38 μm; H_2O_2 = 3.0 M; S/L=0.1 t = 4.0 h; stirring speed = 500 rpm; & T=65 °C	Chemical control	64.0	94.0	This study

work is currently underway to investigate the leaching of Cu-Co ore with a variety of organic acids. Also, since the results obtained have shown that Cu leaching is influenced by internal diffusion. Therefore, in future we intend to further decrease the particle size of the ore sample to improve the leaching efficiency of Cu. In the same vein, we shall take cognisance of the effect of Fe on the sequential leaching of Cu and Co, as well as their recovery from solution with which ever chosen route.

Funding

This work did not receive any specific funding.

CRediT authorship contribution statement

Emmanuel A. Oke: Writing – review & editing, Writing – original draft, Visualization, Validation, Supervision, Software, Methodology, Data curation, Conceptualization. **Herman Potgieter:** Writing – review & editing, Visualization, Validation, Supervision, Project administration, Funding acquisition, Conceptualization. **Fortune Mondlane:** Writing – original draft, Visualization, Validation, Investigation, Formal analysis, Data curation. **Noluthando P. Skosana:** Writing – original draft, Visualization, Validation, Investigation, Formal analysis, Data curation. **Samaneh Teimouri:** Visualization, Software, Methodology, Data curation. **Joseph K. Nyembwe:** Formal Analysis, Visualization, Software, Methodology, Data curation.

Declaration of competing interest

The authors declare that they have no known competing financial interests or personal relationships that could have appeared to influence the work reported in this paper.

Data availability

Data will be made available on request.

Acknowledgement

Emmanuel A. Oke acknowledges the Research Office of the University of the Witwatersrand for the Centennial Postdoctoral Fellowship granted to him between 2023 and 2025.

References

Alvial-Hein, G., Mahandra, H., Ghahreman, A., 2021. Separation and recovery of cobalt and nickel from end of life products via solvent extraction technique: a review. J. Clean. Prod. 297, 126592 https://doi.org/10.1016/j.jclepro.2021.126592.

Astuti, W., Hirajima, T., Sasaki, K., Okibe, N., 2016. Comparison of effectiveness of citric acid and other acids in leaching of low-grade Indonesian saprolitic ores. Miner. Eng. 85, 1–16. https://doi.org/10.1016/j.mineng.2015.10.001.

Barman, P., Dutta, L., Azzopardi, B., 2023. Electric vehicle battery supply chain and critical materials: a brief survey of state of the art. Energies (Basel) 16, 3369. https://doi.org/10.3390/en16083369.

Cai, C., Fajar, A.T.N., Hanada, T., Wakabayashi, R., Goto, M., 2023. Amino acid leaching of critical metals from spent lithium-ion batteries followed by selective recovery of cobalt using aqueous biphasic system. ACS Omega 8, 3198–3206. https://doi.org/10.1021/acsomega.2c06654.

Chen, L., Tang, X., Zhang, Y., Li, L., Zeng, Z., Zhang, Y.i., 2011. Process for the recovery of cobalt oxalate from spent lithium-ion batteries. Hydrometall. 108, 80–86. https://doi.org/10.1016/j.hydromet.2011.02.010.

Chong, S., Hawker, W., Vaughan, J., 2013. Selective reductive leaching of oxidised cobalt containing residue. Miner. Eng. 54, 82–87. https://doi.org/10.1016/j.mineng.2013.04.004.

Clotilde Apua, M., Madiba, M.S., 2021. Leaching kinetics and predictive models for elements extraction from copper oxide ore in sulphuric acid. J. Taiwan Inst. Chem. Eng. 121, 313–320. https://doi.org/10.1016/j.jtice.2021.04.005.

Crundwell, F.K., 2014. The mechanism of dissolution of minerals in acidic and alkaline solutions: Part III. Application to oxide, hydroxide and sulfide minerals. Hydrometall. 149, 71–81. https://doi.org/10.1016/j.hydromet.2014.06.008.

Crundwell, F.K., du Preez, N.B., Knights, B.D.H., 2020. Production of cobalt from copper-cobalt ores on the african copperbelt – an overview. Miner. Eng. 156, 106450 https://doi.org/10.1016/j.mineng.2020.106450.

Dong, B., Wu, J.-H., Wu, J., Zhang, X., Zhai, J., 2019. Solvent extraction process for the selective recovery of copper and cobalt from carrollite leach solution. Metall. Res. Technol. 116, 309. https://doi.org/10.1051/metal/2018104.

Guimarães, L.F., Botelho Junior, A.B., Espinosa, D.C.R., 2022. Sulfuric acid leaching of metals from waste Li-ion batteries without using reducing agent. Miner. Eng. 183, 107597 https://doi.org/10.1016/j.mineng.2022.107597.

Gulley, A.L., 2022. One hundred years of cobalt production in the democratic republic of the congo. Resour. Policy 79, 103007. https://doi.org/10.1016/j.resourpol.2022.103007.

He, L.-P., Sun, S.-Y., Mu, Y.-Y., Song, X.-F., Yu, J.-G., 2017. Recovery of lithium, nickel, cobalt, and manganese from spent lithium-ion batteries using <scp>l</scp> -tartaric acid as a leachant. ACS Sustain. Chem. Eng. 5, 714–721. https://doi.org/10.1021/acssuschemeng.6b02056.

Henckens, M.L.C.M., Worrell, E., 2020. Reviewing the availability of copper and nickel for future generations. The balance between production growth, sustainability and recycling rates. J. Clean. Prod. 264, 121460 https://doi.org/10.1016/j.jclepro.2020.121460.

Hosseini Nasab, M., Noaparast, M., Abdollahi, H., 2020. Dissolution optimization and kinetics of nickel and cobalt from iron-rich laterite ore, using sulfuric acid at atmospheric pressure. Int. J. Chem. Kinet. 52, 283–298. https://doi.org/10.1002/kin.21349.

Hosseinzadeh, M., Entezari Zarandi, A., Pasquier, L.C., Azizi, A., 2021. Kinetic investigation on leaching of copper from a low-grade copper oxide deposit in sulfuric acid solution: a case study of the crushing circuit reject of a copper heap leaching plant. J. Sustainable Metallurgy 7. https://doi.org/10.1007/s40831-021-00408-5.

Jadhao, P.R., Pandey, A., Pant, K.K., Nigam, K.D.P., 2021. Efficient recovery of Cu and Ni from WPCB via alkali leaching approach. J. Environ. Manage. 296, 113154 https://doi.org/10.1016/j.jenvman.2021.113154.

Kundu, T., Senapati, S., Das, S.K., Angadi, S.I., Rath, S.S., 2023. A comprehensive review on the recovery of copper values from copper slag. Powder Technol. 426, 118693 https://doi.org/10.1016/j.powtec.2023.118693.

Li, L., Bian, Y., Zhang, X., Guan, Y., Fan, E., Wu, F., Chen, R., 2018. Process for recycling mixed-cathode materials from spent lithium-ion batteries and kinetics of leaching. Waste Manag. 71, 362–371. https://doi.org/10.1016/j.wasman.2017.10.028.

Li, Y., Chen, Y., Tang, C., Yang, S., He, J., Tang, M., 2017. Co-treatment of waste smelting slags and gypsum wastes via reductive-sulfurizing smelting for valuable metals recovery. J. Hazard. Mater. 322, 402–412. https://doi.org/10.1016/j.jhazmat.2016.10.028.

Li, M., Li, S., 2023. Construction of a bridging network structure by citric acid for environmental heavy metal extraction. ACS Earth Space Chem. 7, 676–684. https://doi.org/10.1021/acsearthspacechem.2c00389.

Li, X.-G., Li, X.-L., Shi, X., Li, G.-Y., Nie, C., Yan, S., Zhu, X., 2024. Innovative closed-loop copper recovery strategy from waste printed circuit boards through efficient ionic liquid leaching. Sep. Purif. Technol. 338, 126530 https://doi.org/10.1016/j.seppur.2024.126530.

Li, H., Oraby, E., Eksteen, J., 2020. Extraction of copper and the co-leaching behaviour of other metals from waste printed circuit boards using alkaline glycine solutions. Resour. Conserv. Recycl. 154, 104624 https://doi.org/10.1016/j.resconrec.2019.104624.

Li, L., Xiao, Y., Lei, Y., Xu, J., Xu, Z., 2023. An approach of cobalt recovery from waste copper converter slags using pig iron as capturing agent and simultaneous recovery of copper and tin. Waste Manag. 165, 1–11. https://doi.org/10.1016/j.wasman.2023.04.019.

Lipman, T.E., Maier, P., 2021. Advanced materials supply considerations for electric vehicle applications. MRS Bull. 46, 1164–1175. https://doi.org/10.1557/s43577-022-00263-z.

Liu, S., He, Y., Xie, H., Ge, Y., Lin, Y., Yao, Z., Jin, M., Liu, J., Chen, X., Sun, Y., Wang, B., 2022. A state-of-the-art review of radioactive decontamination technologies: facing the upcoming wave of decommissioning and dismantling of nuclear facilities. Sustainability 14, 4021. https://doi.org/10.3390/su14074021.

Mohanraj, G.T., Rahman, M.R., Arya, S.B., Barman, R., Krishnendu, P., Singh Meena, S., 2022. Characterization study and recovery of copper from low grade copper ore through hydrometallurgical route. Adv. Powder Technol. 33, 103382 https://doi.org/10.1016/j.apt.2021.12.001.

Mohanty, A., Devi, N., 2023. A review on green method of extraction and recovery of energy critical element cobalt from spent Lithium-Ion Batteries (LIBs). Miner. Process. Extr. Metall. Rev. 44, 52–63. https://doi.org/10.1080/08827508.2021.2017925.

Nagarajan, N., Panchatcharam, P., 2023. Cost-effective and eco-friendly copper recovery from waste printed circuit boards using organic chemical leaching. Heliyon 9, e13806.

Oke, E.A., Osibanjo, O., Raheem, S.A., Oluyinka, O.A., Ibe, K.K., 2023. Metals concentration levels in printed circuit boards of discarded cathode ray tube television: trends over the years. Int. J. Environ. Anal. Chem. 103, 6613–6624. https://doi.org/10.1080/03067319.2021.1958802.

Oke, E.A., Potgieter, H., 2024. Recent chemical methods for metals recovery from printed circuit boards: a review. J Mater Cycles Waste Manag. https://doi.org/10.1007/s10163-024-01944-4.

Olaoluwa, D.T., Baba, A.A., Oyewole, A.L., 2023. Beneficiation of a Nigerian lepidolite ore by sulfuric acid leaching. Mineral Processing and Extractive Metallurgy 132, 134–140. https://doi.org/10.1080/25726641.2023.2216612.

Ozairy, R., Rastegar, S.O., Beigzadeh, R., Gu, T., 2022. Optimization of metal bio-acid leaching from mobile phone printed circuit boards using natural organic acids and H2O2. J Mater Cycles Waste Manag 24, 179–188. https://doi.org/10.1007/s10163-021-01302-8.

Preetam, A., Modak, A., Jadhao, P.R., Naik, S.N., Pant, K.K., Kumar, V., 2022. A comprehensive study on the extraction of transition metals from waste random access memory using acetic acid as a chelating solvent. J. Environ. Chem. Eng. 10, 108761 https://doi.org/10.1016/j.jece.2022.108761.

Raj, T., Chandrasekhar, K., Kumar, A.N., Sharma, P., Pandey, A., Jang, M., Jeon, B.-H., Varjani, S., Kim, S.-H., 2022. Recycling of cathode material from spent lithium-ion batteries: challenges and future perspectives. J. Hazard. Mater. 429, 128312 https://doi.org/10.1016/j.jhazmat.2022.128312.

Salem, A.R., 2023. Efficient leaching process of valuable elements from gibbsite ore materials in talet seleim, southwestern, sinai, egypt using green and ecofriendly lixiviant agent: optimization, kinetic and thermodynamic study. Analytical Chem. Lett. 13, 141–158. https://doi.org/10.1080/22297928.2023.2222281.

Santoro, L., Tshipeng, S., Pirard, E., Bouzahzah, H., Kaniki, A., Herrington, R., 2019. Mineralogical reconciliation of cobalt recovery from the acid leaching of oxide ores from five deposits in Katanga (DRC). Miner. Eng. 137, 277–289. https://doi.org/10.1016/j.mineng.2019.02.011.

Schueler, T.A., de Aguiar, P.F., Vera, Y.M., Goldmann, D., 2021. Leaching of Cu, Zn, and Pb from sulfidic tailings under the use of sulfuric acid and chloride solutions. J. Sustainable Metallurgy 7, 1523–1536. https://doi.org/10.1007/s40831-021-00446-z.

Shengo, M.L., Kime, M.-B., Mambwe, M.P., Nyembo, T.K., 2019. A review of the beneficiation of copper-cobalt-bearing minerals in the democratic republic of congo. J. Sustainable Min. 18, 226–246. https://doi.org/10.1016/j.jsm.2019.08.001.

Steer, J.M., Griffiths, A.J., 2013. Investigation of carboxylic acids and non-aqueous solvents for the selective leaching of zinc from blast furnace dust slurry. Hydrometall. 140, 34–41. https://doi.org/10.1016/j.hydromet.2013.08.011.

Stuurman, S., Ndlovu, S., Sibanda, V., 2014. Comparing the extent of the dissolution of copper-cobalt ores from the DRC region. J. S. Afr. Inst. Min. Metall. 114.

Teimouri, S., Potgieter, J.H., Simate, G.S., van Dyk, L., Dworzanowski, M., 2020. Oxidative leaching of refractory sulphidic gold tailings with an ionic liquid. Miner. Eng. 156, 106484 https://doi.org/10.1016/j.mineng.2020.106484.

Wang, Z., Guo, S., Ye, C., 2016. Leaching of copper from metal powders mechanically separated from waste printed circuit boards in chloride media using hydrogen peroxide as oxidant. Procedia Environ. Sci. 31, 917–924. https://doi.org/10.1016/j.proenv.2016.02.110.

Wang, W.-Y., Yen, C.H., Hsu, J.-K., 2020. Selective recovery of cobalt from the cathode materials of NMC type Li-ion battery by ultrasound-assisted acid leaching and microemulsion extraction. Sep. Sci. Technol. 55, 3028–3035. https://doi.org/10.1080/01496395.2019.1665071.

Wu, J., Ahn, J., Lee, J., 2021. Kinetic and mechanism studies using shrinking core model for copper leaching from chalcopyrite in methanesulfonic acid with hydrogen peroxide. Miner. Process. Extr. Metall. Rev. 42, 38–45. https://doi.org/10.1080/08827508.2020.1795850.

Xu, J., Qin, S., Zheng, C., Wang, J., Yang, B., Qiu, G., Cui, S., Ma, H., 2023. Characterization and optimization of copper-cobalt oxide ores during acid leaching. JOM 75, 5785–5795. https://doi.org/10.1007/s11837-023-06151-4.

Xu, L., Yang, H., Liu, Y., Zhou, Y., 2019. Uranium leaching using citric acid and oxalic acid. J. Radioanal. Nucl. Chem. 321, 815–822. https://doi.org/10.1007/s10967-019-06673-9.

Yang, W., Liu, Y., Li, X., Ma, B., Wang, H., Wang, C., 2023. Selective extraction of cobalt and copper from cobalt-rich copper sulfide ores. Metall. Mater. Trans. B 54, 2332–2346. https://doi.org/10.1007/s11663-023-02834-0.

Zhang, D., Dong, L., Li, Y., Wu, Y., Ma, Y., Yang, B., 2018. Copper leaching from waste printed circuit boards using typical acidic ionic liquids recovery of e-wastes' surplus value. Waste Manag. 78, 191–197. https://doi.org/10.1016/j.wasman.2018.05.036.

Zheng, C., Jiang, K., Cao, Z., Wang, H., Liu, S., Waters, K.E., Ma, H., 2023. Pressure leaching behaviors of copper-cobalt sulfide concentrate from Congo. Sep. Purif. Technol. 309, 123010 https://doi.org/10.1016/j.seppur.2022.123010.